ASIAN JOURNAL OF PHARMACEUTICAL SCIENCES 10 (2015) 203–211

HOSTED BY

ELSEVIER

Available online at www.sciencedirect.com

ScienceDirect

journal homepage: http://ees.elsevier.com/ajps/default.asp

Original Research Paper

Chlorogenic acid loaded chitosan nanoparticles with sustained release property, retained antioxidant activity and enhanced bioavailability

Ilaiyaraja Nallamuthu [a,*], *Aishwarya Devi* [b], *Farhath Khanum* [a,1]

[a] *Biochemistry and Nanosciences Division, Defence Food Research Laboratory (DFRL), Siddharthanagar, Mysore 570011, India*

[b] *National Centre for Nanoscience and Nanotechnology, University of Madras, Chennai 600025, India*

ARTICLE INFO

Article history:
Received 22 August 2014
Received in revised form
15 September 2014
Accepted 26 September 2014
Available online 19 December 2014

Keywords:
Chlorogenic acid
Chitosan
Nanoencapsulation
Antioxidant activity
In vitro release kinetics
Pharmacokinetic analysis

ABSTRACT

In this study, chlorogenic acid (CGA), a phenolic compound widely distributed in fruits and vegetables, was encapsulated into chitosan nanoparticles by ionic gelation method. The particles exhibited the size and zeta potential of 210 nm and 33 mV respectively. A regular, spherical shaped distribution of nanoparticles was observed through scanning electron microscopy (SEM) and the success of entrapment was confirmed by FTIR analysis. The encapsulation efficiency of CGA was at about 59% with the loading efficiency of 5.2%. *In vitro* ABTS assay indicated that the radical scavenging activity of CAG was retained in the nanostructure and further, the release kinetics study revealed the burst release of 69% CGA from nanoparticles at the end of 100th hours. Pharmacokinetic analysis in rats showed a lower level of C_{max}, longer T_{max}, longer MRT, larger AUC_{0-t} and $AUC_{0-\infty}$ for the CGA nanoparticles compared to free CGA. Collectively, these results suggest that the synthesised nanoparticle with sustained release property can therefore ease the fortification of food-matrices targeted for health benefits through effective delivery of CGA in body.

1. Introduction

Chlorogenic acid (CGA) is a polyphenolic antioxidant distributed widely in fruits like apple, pears, berries, plum and vegetables like sweet potato, lettuce, spinach, coffee beans, tea, etc. [1,2]. Structurally, it is the esters of certain *trans*-cinnamic acids (caffeic, ferulic and p-coumaric acids) and quinic acid [3]. Out of many forms, 5-caffeoylquinic acid is most predominant form of CGA in plants. The antioxidant property of CGA is attributed to its double bond conjugated catechol structure of the phenyl ring. Green coffee is remarkably the richest sources of CGA with the content of 4–14% [4]. Several recent reports on cell lines and animal studies have shown its pharmacological properties that include anti-obese [5], anti-inflammatory [6,7], neuroprotective [8,9], anti-diabetic [10], antioxidant [11],

* *Corresponding author*. Biochemistry and Nanosciences Division, Defence Food Research Laboratory (DFRL), Siddharthanagar, Mysore 570011, India. Tel.: +91 821 2473290; fax: +91 821 2473468.
E-mail address: nilaiyaraja@gmail.com (I. Nallamuthu).
[1] Tel.: +91 821 2473290; fax: +91 821 2473468.

Peer review under responsibility of Shenyang Pharmaceutical University.
http://dx.doi.org/10.1016/j.ajps.2014.09.005

anti-cancerous [12], radio protective [13], neuroprotective properties, and also for treating Alzheimer's disease [14] etc. Furthermore, CGA inhibit oxidation of LDL and therefore protect against cardiovascular diseases.

There is a growing interest in the dietary supplementation of CGA as a nutraceutical agent in food formulations due to its various medicinal properties. Despite its safety and effectiveness the use of CGA is limited by its low bioavailability and stability [15,16]. In intestine, the CGA either absorbed as an intact form or hydrolysed forms of caffeic acid and quinic acid. After ingestion, only a one third of CGA absorbed from gastrointestinal tract reaches blood circulation [17]. Moreover, CGA can also undergo enzymatic oxidation in many food processes to quinines by polyphenol oxidase and while roasting of green coffee beans it forms CGAs lactones and shikimates by dehydration process [18]. Recently it was reported that the thermal processing of foods containing a high concentration CGA facilitate the formation of acrylamide [19]. Other oxidative process in foods may also result in the formation of a reactive electrophilic chlorogenoquinone, and can also undergo transesterification reaction during storage/processing of foods [20]. Therefore, as an effective strategy to overcome such problems, CGA can be encapsulated in a variety of polymers [21].

Encapsulation technique has emerged as a promising delivery system in the recent past and has successfully been applied for a number of pharma drugs [22]. In food industries, it is being targeted to improve poorly soluble and bioavailabile phytocompounds. Also the targetability, slow release property and stability of the substances can be greatly modified [23]. Upon ingestion, the nanoparticles in the fortified foods get adhered to the mucosa of GIT which is a prerequisite before transit into the body, and then transported via circulation to different organs. Such system could prolong the therapeutic effect of nutraceuticals at their specific target sites [24]. For such entrapment purposes, polymers such as proteins, lipids, carbohydrates can serve as a wall material/carrier material depending on the nature of substances to be encapsulated. Chitosan is one of the widely used cationic polysacchrides due to its nontoxicity, biocompatibility, biodegradability with permeation enhancing properties [25,26].

The objective of the present study was to prepare and characterize the chlorogenic acid loaded chitosan nanoparticles with preserved antioxidant activity, controlled release property and enhanced bioavailability.

2. Materials and methods

2.1. Chemicals

Chitosan with a deacetylation degree of 86.6% (catalog no. LMW 448869), sodium tripolyphosphate, chlorogenic acid, and 2,2-azinobis(3-ethylbenzothiazoline-6-sulfonic acid) were purchased from Sigma Aldrich Chemical Co. Acetic acid, methanol, formic acid were purchased from Loba Chemie, Mumbai (India).

2.2. Preparation of chlorogenic acid loaded chitosan nanoparticles (CNP)

The nanoparticles were prepared according to the procedure reported by Calvo et al. [27], based on the ionic gelation of chitosan with TPP anions. In brief, chitosan was dissolved in acetic acid aqueous solution at various concentrations and the concentration of acetic acid in aqueous solution was, in all cases 1.75 times that of chitosan. Under magnetic stirring at room temperature, 3 ml of TPP aqueous solution at various concentrations was added into 5 ml of chitosan solutions using a peristaltic HPLC pump (Neulab, India) with 0.2 ml/min flow rate. The final concentration of chitosan and TPP in nanoparticle suspensions were 1.5, 2, 2.5, 3 mg/ml and 0.5, 0.6 and 0.7 mg/ml respectively. The concentration of acetic acid in aqueous solution was 1.75 times the final concentration of chitosan. Nanoparticles were separated by centrifugation followed by lyophilisation of nanoparticles and stored at 4 °C until further use.

2.3. Characterization of nanoparticles

2.3.1. Particle size and zeta potential

The sizes and zeta potential of the CNP were measured with a Malvern Zetasizer Nano ZS (Malvern Instruments Ltd., Malvern, U.K.). The particle size distribution of the nanoparticles is reported as a polydispersity index (PDI). All measurements were performed in triplicates. 3 ml of sample was taken in a cuvette and was analysed at 25 °C with at an angle of 90°.

2.3.2. Scanning electron microscope (SEM)

Particle morphology was examined by scanning electron microscope (SEM) (Hitachi). The CNP were separated by centrifugation at 40,000 g for 30 min. The supernatant was decanted and the pellet was freeze dried with the lyophilizer (LSI, India) and was examined by SEM at an accelerating voltage of 15.0 kV. One drop of nanoparticles was placed on a graphite surface and when the sample had dried then it was coated with gold using ion sputter.

2.3.3. FTIR and DSC

FTIR spectra of chitosan, chlorogenic acid, sodium tripolyphosphate and CNP were obtained to detect the functional groups using FTIR spectrometer (Thermoelectron Corporation, USA). The samples were ground finely with potassium bromide and were then pressed mechanically to form a translucent disc. These samples were scanned from 4000 to 400 cm^{-1} wave number.

Differential scanning calorimetry (DSC, TA Instruments) monitors heat effects associated with phase transitions and chemical reactions as a function of temperature. The difference in heat flow to the sample and a reference was recorded. DSC was calibrated using an empty aluminium pan as a standard and samples weighing about 3–6 mg were heated in sealed aluminium pans. Thermogram was recorded covering a range of 25–300 °C at a heat rate of 10 °C/min, under dry nitrogen condition.

2.4. Encapsulation (EE) and loading efficiency (LE)

The EE of CGA was determined by the separation of nanoparticles from the aqueous medium containing non-associated chlorogenic acid using ultracentrifugation at 40,000 *g*, 4 °C for 30 min. The amount of free chlorogenic acid in the supernatant was measured by high performance liquid chromatography

(JASCO Pu-1580 HPLC System). A 250 × 4.6 mm column (C_{18} column; Waters) was used as a solid phase. The mobile phase consisted of 40% methanol and 0.06% formic acid. The system was run isocratically with a flow rate of 0.8 ml/min 20 μl of sample was injected into the column and the quantification was done at 327 nm using Photo diode array detector (BORWIN software). All measurements were performed in triplicate. The encapsulation efficiency (EE) and Loading capacity (LC) of CGA were calculated as below.

EE (%) = (weight of CGA in nanoparticles × 100)/weight of total CGA

LC (%) = (weight of CGA in nanoparticle × 100)/weight of nanoparticles CGA

2.5. *Effect of pH on nanoparticles*

pH is the one of the most important factor that affects zeta potential and size of the nanoparticle. To evidence these changes, pH titration was done using DLS (Malvern Zetasizer Nano ZS) and the change in pH was plotted as a function of size and zeta potential. The nanoparticles were autotitrated using 0.1 N NaOH in order to find out the isoelectric point of the sample up to pH 10.

2.6. *In vitro antioxidant assay*

ABTS is a free radical which oxidises the antioxidants. It is a coloured reagent (bluish green) and when the antioxidant is added it turns colourless. The intensity of the colour change is measured as the function of antioxidant activity [28]. The antioxidant activity of encapsulated chlorogenic acid was evaluated by the 2, 2-azinobis (3-ethylbenzothiazoline-6-sulfonic acid) ABTS radical scavenging assay. 140 mM/L ABTS stock solution was diluted in water to 14 mM concentration. 500 μl of 14 mm ABTS dilution and 500 μl of 4.9 mM potassium persulfate stock solution were mixed in a 1.5 ml tube and then left to stand in the dark and at room temperature for at least 12 h. The ABTS was then diluted with sample buffer to an absorbance of 0.700 at 734 nm before use. After the addition of 900 μl of diluted ABTS solution to 100 μl sample, the absorbance of sample (A_{sample}) was taken exactly after 6 min, and the absorbance of sample buffer blank ($A_{control}$) was run in each assay. The absorbance at 734 nm was recorded by means of UV-Vis spectrometry (Shimadzu, Japan). All determination was carried in triplicates. IC_{50} of the antioxidant was calculated. The radical scavenging activity (RSA) was calculated using the equation;

$$RSA\ (\%) = [(A_{control} - A_{sample})/A_{control}] \times 100$$

2.7. *In vitro release kinetics*

50 mg of nanoparticles separated by ultracentrifugation was dissolved in 3 ml of phosphate buffer saline (pH 7.4) and 0.1 M HCl. This was placed in a dialysis membrane with a molecular cut off range of 7 kDa (Cat no: 68700, Pierce Make) at 37 °C. The sample containing dialysis tube was immersed in 75 ml of phosphate buffer under magnetic stirring condition for 100 h. At regular intervals of time, 2 ml of the released sample was removed and replaced with 2 ml of buffer. The amount of chlorogenic acid in the release medium was quantified by HPLC.

2.8. *In vivo pharmacokinetics*

Wistar male (120 g) rats were kept in an environmentally controlled animal facility operating on a 12 h dark/light cycle at 24 °C and 55% humidity. 18 rats were randomly divided into two groups (9 animals each) and they were fasted for 14–15 h prior to CGA administration. Control group was orally administered with 100 mg/kg of free CGA and the treatment group was given an equivalent dose of nanoparticles. Blood was collected from bleeding of tail vein at 0.5, 1, 2, 3, 4, 5, 6, 12 and 24 h following oral administration. CGA was determined by high performance liquid chromatography (HPLC) after extraction from the blood plasma. Briefly, to 50 μl of plasma 50 μl of enzyme solution containing 500 U of β-glucuronidase and 25 U of sulfatase was added and incubated at 37 °C for 50 min and to this 900 μl of methanol/acetic acid (100:5, v/v) were added. The mixture was vortexed for 30 s, sonicated for 30 s, again vortexed for 30 s, and centrifuged for 5 min at 4 °C and 5000 g. The supernatant was diluted with water (1:1 v/v), and 20 μl was injected onto an HPLC column for quantification.

Pharmacokinetics parameters were determined by non-compartmental analysis using phoenix software, Certara. The data were presented for area under the curve (AUC), peak concentration (C_{max}), time of peak concentration (T_{max}), and mean residence time (MRT).

2.9. *Thermal and storage stability*

For the thermal stability studies, 3 ml of nanoparticles solution was transferred into 9 test tubes. Three test tubes were heated for 5, 10 and 15 min at 80, 100 and 120 °C respectively. The change in the physicochemical properties of the chlorogenic acid loaded nanoparticles after heat treatment was done by measuring the particle size and zeta potential [29]. For storage stability studies, three test tubes were filled with 5 ml of the nanoparticle solution and were stored at room temperature for one month. The stability of the nanoparticle was done by measuring the size using DLS.

2.10. *Statistical analysis*

Results from replicates were expressed as mean ± standard deviation. Analysis of variance was performed using the *t*-test. The *p* values less than 0.05 were considered as significant different.

3. Results and discussion

3.1. *Preparation and characterisation of CGA nanoparticles*

Chitosan is one of the widely used encapsulating agent and several reports on chitosan based encapsulation have been

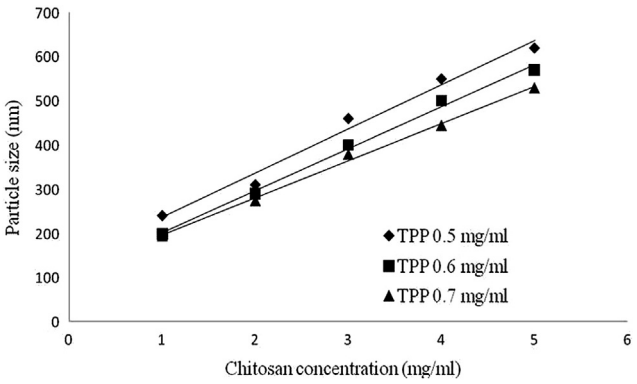

Fig. 1 – Size of the nanoparticles at various concentrations of chitosan and TPP.

published recently for polyphenolic compounds including quercetin [30], gallic acid [31], catechin and epigallocatechin gallate [32], procyanidins [33], ferulic acid [34] and tea polyphenols [35]. In our study, chlorogenic acid was encapsulated into this polymer by ionic gelation method. The effect of various concentrations of chitosan and TPP on nanoparticle size was evaluated. Results indicated that the mean size of nanoparticles increased with an increase in concentration of chitosan from 1 to 5 mg/ml with a linear relationship (Fig. 1). The lowest mean diameter of 210 nm size was obtained at a chitosan concentration of 1.0 mg/ml and a TPP concentration of 0.7 mg/ml. The ratio of chitosan/TPP was 1.5:1 and this is an important critical fabricating parameters in encapsulation. The size distribution profile of the nanoparticles for the lowest concentration is presented in Fig. 2. The particle size of the chitosan nanoparticle for the catechin [36] and sylicylic acid [37] was reported to be 130 ± 5 nm and 150–370 nm respectively. The zeta potential of nanoparticle was positively charged at about 33 mV (Fig. 3). In general, particle charge is a stability determining factor and a zeta potential of >+30 mV and <−30 mV is ideal for a physical stability of any suspension. When chitosan and TPP were mixed in acetic acid solution, they spontaneously formed compact nanocomplexes with an overall positive surface charge, and the density of the surface charge was reflected in the measured zeta potential values. It was also observed that zeta potential increased linearly with increasing chitosan concentration. A similar range of zeta potentials (>+30 mV) have been obtained for salicylic acid and gentamicin-loaded nanoparticles in earlier published reports [38].

At lowest concentration of CGA (0.1 mg/ml), the encapsulation efficiency (EE) was 59% with the particle size of 210 nm. As the concentration increased to 0.5 mg/ml, the EE was reduced to 45% and the mean particle size was increased to 255 nm (Table 1).

3.1.1. *SEM and FT-IR analysis*

The morphology and size distribution of the prepared nanoparticles were examined under scanning electron microscope. The shape of the nanoparticles was found to be spherical, homogeneous in shapes with smooth surface (Fig. 4). The dimension of the nanoparticle was ~250 nm suggesting nanodimension of the encapsulated CGA. These nanosized particles are likely to improve CGA bioavailability through higher absorption in body.

The FTIR spectra of nanoparticle and their ingredients are presented in Fig. 5. Absorption in this infrared region is due to changes in vibrational energy. The essential requirement for a substance to absorb in these regions is that the vibrations in the molecule must give rise to an unsymmetrical charge distribution. The region 1400–650 cm^{-1} is known as the finger print region and therefore this region usually checked for identification of functional groups. It is also associated with vibrational (and rotational) energy changes of the molecular skeleton, and so is a characteristic of the compound under study.

The characteristic absorption peak of chitosan was observed at 3000–3500 cm^{-1} (OH, NH2) [39]. The peak for asymmetric stretch of C–O–C is found at around 1150 $cm^{-1}$and CH stretching at 2874 cm^{-1}. The peak at 1317 cm^{-1} belongs to the C–N stretching vibration of type I amine. The peaks for N–H bending vibration of amine I at 1589 cm^{-1} and the amide II carbonyl stretch at 1650 cm^{-1} in nanoparticles shifted to 1629 cm^{-1} and 1529 cm^{-1}, respectively. The crosslinked chitosan also show a P=O peak at 1151.1 cm^{-1}. These results can be attributed to the linkage between phosphoric group of TPP and ammonium group of chitosan in nanoparticles.

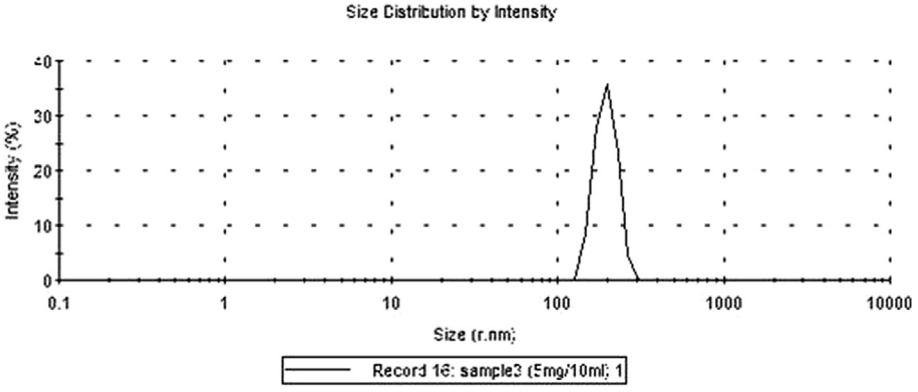

Fig. 2 – Particle size distribution of CGA loaded chitosan nanoparticle at 1 mg/ml of chitosan and 0.7 mg/ml of TPP concentration.

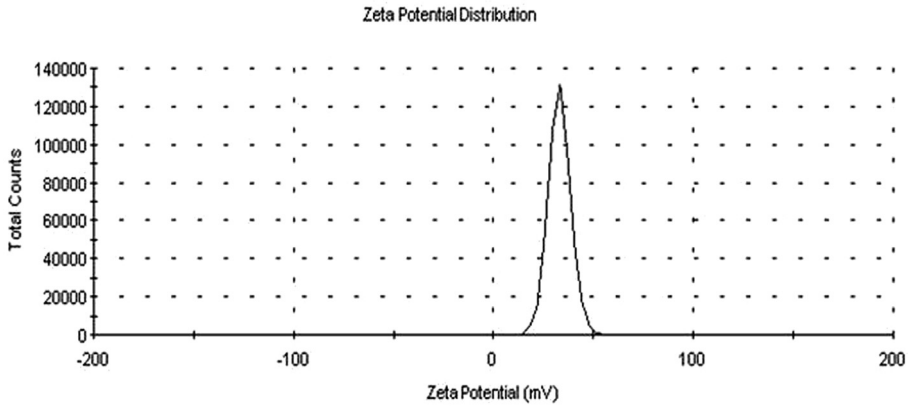

Fig. 3 – Zeta potential distribution of CGA loaded chitosan nanoparticle at 1 mg/ml of chitosan and 0.7 mg/ml of TPP concentration.

Table 1 – Effect of various concentration of chlorogenic acid on particle size and zeta potential of the nanoparticles at the chitosan concentration of 1 mg/ml and TPP concentration of 0.7 mg/ml. All data are mean ± SD of triplicate.

Chlorogenic acid (mg/ml)	Particle size (nm)	Polydispersity index	Zeta potential (mV)	Encapsulation efficiency (%)
0.1	210 ± 8.0	0.35	33 ± 0.9	59 ± 0.2
0.2	225 ± 9.5	0.32	34 ± 0.6	51 ± 0.3
0.3	250 ± 7.5	0.23	30 ± 0.5	48 ± 0.1
0.4	146 ± 5.0	0.43	29 ± 0.7	50 ± 0.5
0.5	255 ± 10.1	0.41	27 ± 0.6	45 ± 0.3

The broad absorption band at 3314.8 is attributed to the O–H vibration, 1686 to the mixed esters and carboxyl C–O vibration, 1638, 1600, 1516, 1442 to the aromatic ring stretch vibration, 1288, 1181, to the carboxylic C–O–C vibration. These results are in consistent with earlier report of Wei et al., [40].

3.1.2. *DSC study*

DSC analysis is used as a tool to confirm the crystal transformation of the nanoparticles. The DSC curves of TPP, CGA, Chitosan and nanoparticles are shown in Fig. 6. TPP and CGA give rise to a sharp peak at 207 °C and 205 °C respectively corresponding to the melting point of crystalline region. The chitosan polymer showed a peak at 191.6 °C and nanoparticles at 200 °C. A shift in the melting point may be due to the interaction of chitosan with chlorogenic acid. Since the shift is not too far, it can be assumed that the encapsulation process did not affect the structure and properties of chitosan polymer.

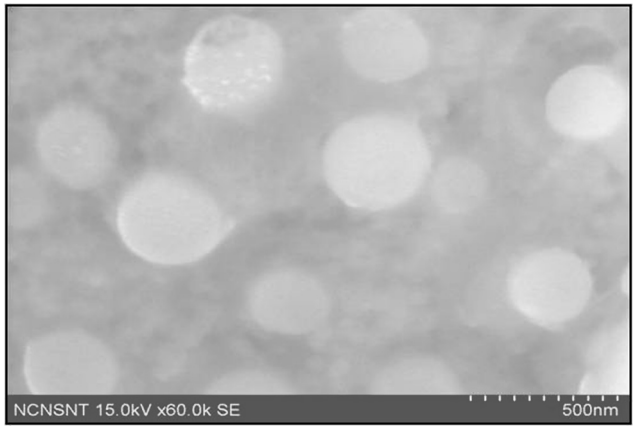

Fig. 4 – SEM image of CGA loaded chitosan nanoparticles.

3.2. *Encapsulation efficiency and loading efficiency*

The encapsulation (EE) and loading capacity (LC) of the chlorogenic acid were determined by HPLC method with the retention time of 20.0 min. EE and LC were found to be 59 and 5.2% respectively. These are the important parameters as far as the delivery of any nureaceuticals/drug is concerned. Previous studies have shown that encapsulation efficiency is greatly influenced by the molecular weight of chitosan used [41]. Depending upon the drug polymer interaction the EE can vary on an average from 10% to 65% or more and in case of gemcitabine-loaded chitosan nanoparticle the EE was reported to be 63% [42]. The loading ability of CGA into the nanoparticles may involve mechanism like electrostatic interaction, encapsulation and adsorption.

3.3. *Effect of pH on nanoparticle*

Fig. 7 shows the titration graph of the nanoparticle from acidic (pH 4) to alkaline (pH 10). When the pH of the suspension increased by incremental addition of NaOH the zeta potential of the nanoparticle steeply decreased from +30 mV to −5 mV and the size drastically increased from 170 nm to 1800 nm. The change in zeta potential may be due to the addition of alkali, and therefore the particles tend to acquire more negative charges. In titration, a point will be reached where the

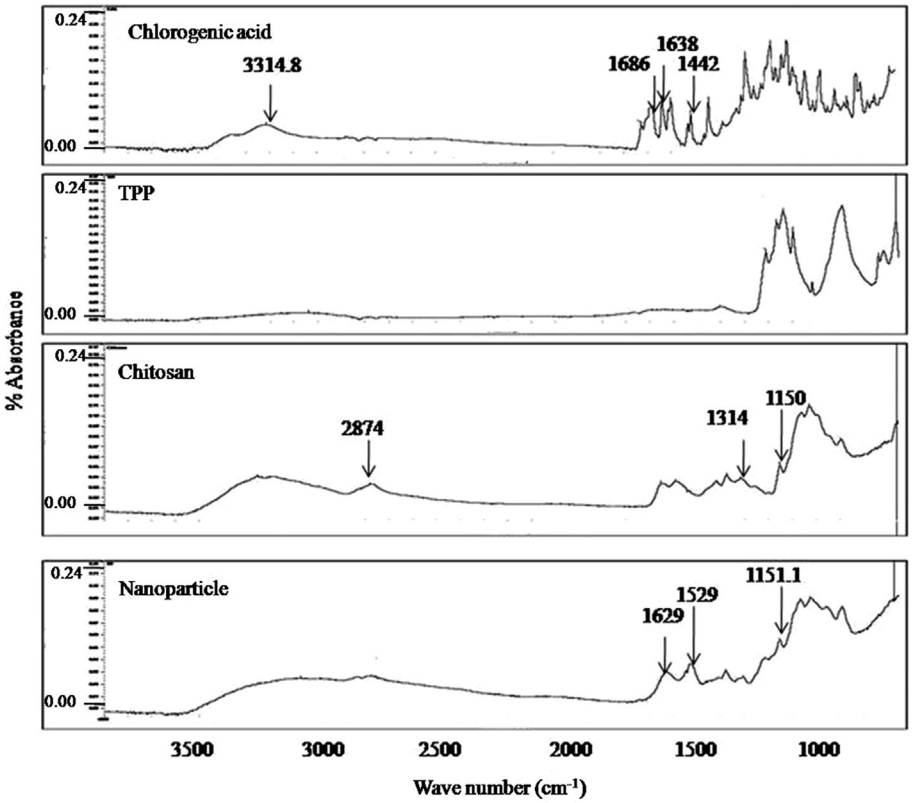

Fig. 5 – FTIR spectra of chlorogenic acid, TPP, chitosan and nanoparticles.

positive charge is completely neutralised by the negative charges. This point is known as the isoelectric point (Pi) which is defined as the pH at which the net charge of the particle is zero and is very important from a practical consideration. Pi of the nanoparticle was found to be at pH 7.66 indicating the least stability of these nanoparticles at this point.

3.4. *In vitro antioxidant assay*

ABTS radical cation decolorization assay is a widely used method for the assessment of the antioxidant activity of various substances. The IC_{50} value of any antioxidant refers to the minimum amount of the substances that is required to

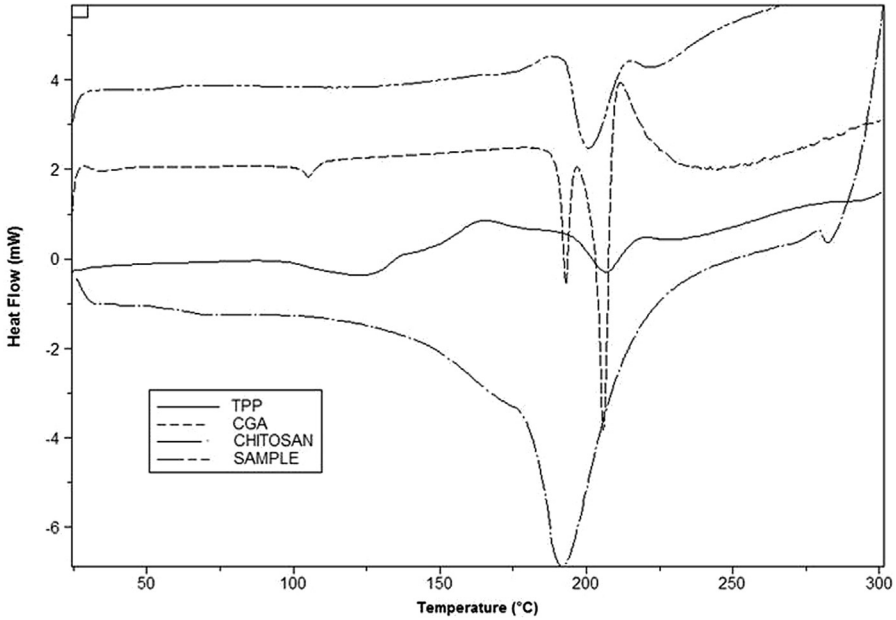

Fig. 6 – DSC thermogram of TPP, CGA, chitosan and nanoparticles.

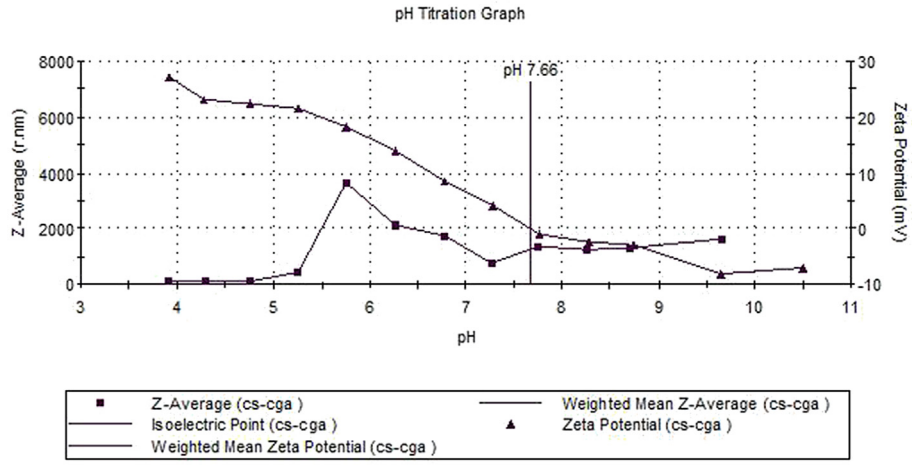

Fig. 7 – Effect of pH on particle size and zeta potential of the chitosan nanoparticles.

scavenge 50% of the radicals generated through *in vitro* system. The scavenging activity of the encapsulated antioxidant expressed in terms of percentage of radical scavenging activity increased with increasing concentration of nanoparticles. The IC_{50} value of the encapsulated CGA (92 ± 5 μg/ml) was comparable to that of an equivalent amount unencapsulated CGA (89 ± 3 μg/ml) indicating that sustained free radical scavenging activity of CGA was retained in the synthesised nanoparticles. Amorim et al. [43], earlier reported a similar preserved antioxidant activity for idebenone-loaded nanoparticles.

3.5. *Release kinetics in vitro*

The release profile of CGA from nanoparticles was investigated at 37 °C over a period of 100 h (Fig. 8). 0.1 M HCl and PBS were used to simulate the stomach and intestine conditions respectively. The release of CGA was rapid in PBS than that of HCl in the same period of time. It also showed a controlled release pattern characterized by a fast initial release (25%) during the first 10 h, followed by slower and continuous release (69%) till 100 h. This kind of continuous and slow release has been reported earlier for drugs such as acetylsalicylic acid, probucol [44]. The release mechanism of drug may involve either by drug molecules diffusion or by polymer matrix degradation *per se* [45]. The initial burst release of drug results from those drug molecules dispersing close to the nanoparticle surface. Since the size of CGA is much smaller than that of the nanoparticles, it can diffuse easily through the surface or pores of nanoparticles quickly. Due to the hydrophilic nature of chitosan, the release medium can easily penetrates into the particle and dissolves the entrapped CGA to outside. Hu et al. [46], studied and shown the controlled release profile of entrapped tea catechins in CS-TPP nanoparticles.

3.6. *In vivo pharmacokinetics analysis*

The mean plasma concentration–time curve after single-dose administration of CGA in rats is presented in Fig. 9 and the relevant pharmacokinetic parameters are listed in Table 2. Encapsulated CGA had significantly lower level of C_{max}, longer T_{max}, longer MRT, larger AUC_{0-t} and $AUC_{0-\infty}$ than that of free CGA ($p < 0.01$). These results indicated that encapsulated CGA had the slower and sustained release of CGA over longer duration, and therefore the bioavailability is more upon oral administration.

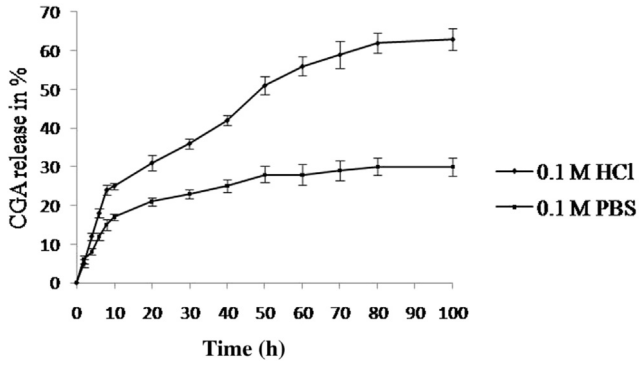

Fig. 8 – *In vitro* release kinetics of CGA from nanoparticles in 0.1 M HCl and 0.1 M Phosphate buffer saline (PBS).

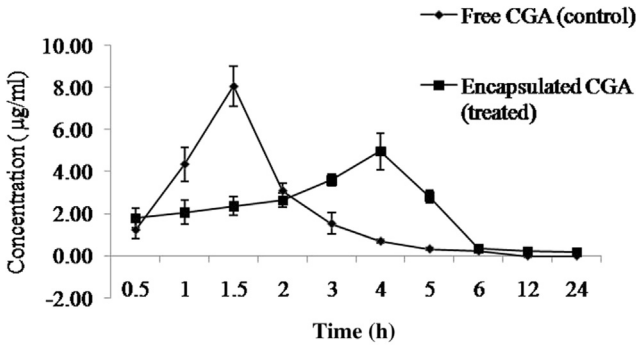

Fig. 9 – Mean plasma concentration – time curve of CGA in control and treatment group after single oral administration in rats (mean ± SD, 100 mg/kg, $n = 9$).

Table 2 – The *in vivo* pharmacokinetic parameters of free CGA (control) and encapsulated CGA (treated) after single oral administration in rats (mean ± SD, $n = 9$).

Parameters (units)	Control group	Treated group
T_{max} (h)	1.5 ± 0.3	4.0 ± 0.5
C_{max} (μg/ml)	8.07 ± 0.97	4.97 ± 0.86
MRT (h)	2.32 ± 0.7	5.38 ± 0.9
AUC_{0-t} (μg.h/ml)	12.74 ± 2.5	21.07 ± 3.4[a]
$AUC_{0-\infty}$ (μg.h/ml)	13.14 ± 2.9	21.01 ± 4.1[a]

[a] $P < 0.01$ versus control group.

3.7. *Thermal and storage stability*

The change in size and zeta potential of nanoparticles during heat treatment at 80, 100 and 120 °C is shown in Fig. 10a and b. There was a rapid reduction in the size and zeta potential of the nanoparticles during the initial 5 min of heating at all the temperatures and then later up to 15 min period of time the effect was minimal with gradual reduction on size and zeta. Heat treatment might have affected the adsorption of chlorogenic acid onto the surface as well as the cross-linking structure related to the formation of the layer. As a result, particle size was reduced and the positive charge on the surface was also changed which in turn might have caused lowering of the zeta potential. This mechanism proceeds relatively rapidly with the rise in temperature. With further heat treatment, however, particle size and zeta potential were maintained within a regular range, probably because the matrix structure in which chlorogenic acid and chitosan were combined through ionic gelation inside the particles was more stable than the particle surface. The effect of heat on nanoparticles was similar to the earlier report of Jang et al. [29], for the encapsulated vitamin-C.

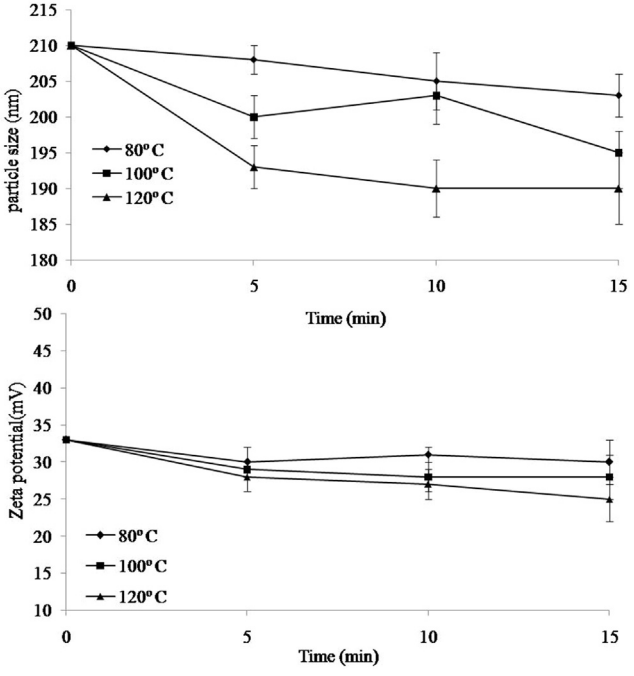

Fig. 10 – Effect of heat treatment at 80, 100 and 120 °C on the particle size and zeta potential of CGA nanoparticles.

Further, the stability of the nanoparticle at room temperature was studied for a month upon storage. It was found to be almost stable with respect to particle size as well as zeta potential of the particles indicating the overall stability of the nanoparticles in aqueous environment (data not shown).

4. Conclusion

Encapsulation of CGA into chitosan was successfully carried out in this study by ionic gelation method. The prepared nanoparticles showed a controlled release profile and a preserved antioxidant activity under *in vitro* conditions. They also showed a considerable heat stability demonstrating its usage in various types of thermally processed foods. Nanoparticles are well-known to transport bioactive compounds across the mucosal barrier and therefore the synthesized nanoparticles with increased bioavailability from the present study can be a suitable carrier for better delivery of CGA in food and pharmaceutical applications.

Acknowledgement

This work was financially supported by DRDO, India. The authors are also thankful to the Director, DFRL, and Mysore for providing technical support and valuable suggestions.

REFERENCES

[1] Farah A, Monterio M, Donangelo CM, et al. Chlorogenic acid from green coffee extract is highly bioavailable in humans. J Nutr 2008;138:2309–2315.
[2] Zhenga W, Clifford MN. Profiling the chlorogenic acids of sweet potato (*Ipomoea batatas*) from China. Food Chem 2008;106:147–152.
[3] Clifford MN, Johnston K, Knigh S, et al. Hierarchical scheme for LC-MS identification of chlorogenic acids. J Agric Food Chem 2003;51:2900–2911.
[4] Perrone D, Faraha A, Donangeloa CM, et al. Comprehensive analysis of major and minor chlorogenic acids and lactones in economically relevant Brazilian coffee cultivars. Food Chem 2008;106:859–867.
[5] Cho A, Jeon S, Kim M, et al. Chlorogenic acid exhibits anti-obesity property and improves lipid metabolism in high-fat diet-induced-obese mice. Food Chem Toxicol 2010;48(3):937–943.
[6] Shan J, Fu J, Zhao Z, et al. Chlorogenic acid inhibits lipopolysaccharide-induced cyclooxygenase-2 expression in RAW 264.7 cells through suppressing NF-κB and JNK/AP-1 activation. Int Immunopharmacol 2009;9:1042–1048.
[7] Shin HS, Satsu H, Bae M, et al. Anti-inflammatory effect of chlorogenic acid on the IL-8 production in Caco-2 cells and the dextran sulphate sodium-induced colitis symptoms in C57BL/6 mice. Food Chem 2015;168:167–175.
[8] Bouayed J, Rammal H, Dicko A, et al. Chlorogenic acid, a polyphenol from *Prunus domestica* (Mirabelle), with coupled anxiolytic and antioxidant effects. J Neurol Sci 2007;262:77–84.
[9] Li Y, Shi W, Li Y, et al. Neuroprotective effects of chlorogenic acid against apoptosis of PC12 cells induced by

methylmercury. Environ Toxicol Pharmacol 2008;26(1):13–21.
[10] Karthikesan K, Pari, Menon VP. Antihyperlipidemic effect of chlorogenic acid and tetrahydrocurcumin in rats subjected to diabetogenic agents. Chem Biol Interact 2010;188:643–650.
[11] Sato Y, Itagaki S, Kurokawa T, et al. *In vitro* and *in vivo* antioxidant properties of chlorogenic acid and caffeic acid. Int J Pharm 2011;403(17):136–138.
[12] Kasai H, Fukada S, Yamaizumi Z, et al. Action of chlorogenic acid in vegetables and fruits as an inhibitor of 8-hydroxydeoxyguanosine formation *in vitro* and in a rat carcinogenesis Model. Food Chem Toxicol 2000;38:467–471.
[13] Cinkilic N, Cetintas SK, Zorlu T, et al. Radioprotection by two phenolic compounds: chlorogenic and quinic acid, on X-ray induced DNA damage in human blood lymphocytes *in vitro*. Food Chem Toxicol 2013;53:359–363.
[14] Lee B, Choi H, Jeong C, et al. Chlorogenic acid ameliorates brain damage and edema by inhibiting matrix metalloproteinase-2 and 9 in a rat model of focal cerebral ischemia. Eur J Pharmacol 2012;689:89–95.
[15] Azua K, Ippoushi K, Nakayama M, et al. Absorption of chlorogenic acid and caffeic acid in rats after oral administration. J Agric Food Chem 2000;48:5496–5500.
[16] Shi G, Rao L, Yu H, et al. Yeast-cell-based microencapsulation of chlorogenic acid as a water-soluble antioxidant. J Food Eng 2007;80:1060–1067.
[17] Olthof MR, Hollman PCH, Katan MB. Chlorogenic acid and caffeic acid are absorbed in humans. J Nutr 2001;131:66–71.
[18] Jaiswal R, Matei MF, Subedi P, et al. Does roasted coffee contain chlorogenic acid lactones or/and cinnamoylshikimate esters? Food Res Int 2014;61:214–227.
[19] Cai Y, Zhang Z, Jiang S, et al. Chlorogenic acid increased a crylamide formation through promotion of HMF formation and 3-aminopropionamide deamination. J Hazard Mat 2014;268:1–5.
[20] Villegas RJA, Shimokawa T, Okuyama H, et al. Purification and characterization of chlorogenic acid: chlorogenate caffeoyl transferase in sweet potato roots. Phytochemistry 1987;26:1577–1581.
[21] Fang Z, Bhandari B. Encapsulation of polyphenols – a review. Trends Food Sci Technol 2010;21(10):510–523.
[22] Wu Y, Yang W, Wang C, et al. Chitosan nanoparticles as a novel delivery system for ammonium glycyrrhizinate. Int J Pharm 2005;295:235–245.
[23] Tan CP, Nakajima M. β-carotene nanodispersions. Preparation, characterisation and stability evaluation. Food Chem 2005;92:661–671.
[24] Allemenn E, Gurny R, Deolker E. Drug loaded nanoparticles: preparation methods and drug targeting tissues. Eur J Pharm Biopharm 1993;39:173–191.
[25] Ravikumar MNV. A review of chitin and chitosan applications. React Funct Polym 2000;46:1–27.
[26] Agnihotri SA, Mallikarjuna NN, Aminabhavi TM. Recent advances on chitosan-based micro- and nanoparticles in drug delivery. J Control Release 2004;100:5–28.
[27] Calvo P, Remunan-Lopez C, Vila-Jato JL, et al. Chitosan and chitosan/ethylene oxide-propylene oxide block copolymer nanoparticles as novel carriers for proteins and vaccines. Pharm Res 1997;14:1431–1436.
[28] Braca A, Tommasi ND, Bari LD, et al. Antioxidant principles from *Bauhinia tetrapotensis*. J Nat Prod 2001;64:892–895.
[29] Jang K, Lee HG. Stability of chitosan nanoparticles for L-ascorbic acids during heat treatment in aqueous solution. J Agric Food Chem 2008;56:1936–1941.
[30] Kumari A, Yadav SK, Pakade YB, et al. Development of biodegradable nanoparticle for delivery of quercetin. Colloids Surf B 2010;80:184–192.
[31] Rosa CG, Borges CD, Zambiazi RC, et al. Microencapsulation of gallic acid in chitosan, β-cyclodextrin and xanthan. Ind Crops Prod 2013;46:138–146.
[32] Dube A, Nicolazzo JA, Larson I. Chitosan nanoparticle enhance the plasma exposure of – epigallocatechin gallate in mice through an enhancement in intestinal stability. Eur J Pharm Sci 2011;44:422–426.
[33] Zou T, Percival SS, Cheng Q, et al. Preparation, characterization, and induction of cell apoptosis of cocoa procyanidins-gelatin-chitosan nanoparticle. Eur J Pharm Biopharm 2012;82:36–42.
[34] Woranuch S, Yoksan R. Preparation, characterization and antioxidant property of water-soluble ferulic acid grafted chitosan. Carbohydr Polym 2013;96(2):495–502.
[35] Liang J, Li F, Fang Y, et al. Synthesis, characterization and cytotoxicity studies of chitosan -coated tea polyphenols nanoparticles. Colloids Surf B 2011;82:297–301.
[36] Dudhani AR, Kosaraju SL. Bioadhesive chitosan nanoparticles: preparation and characterization. Carbohydr Polym 2010;81:243–251.
[37] Dong Y, Ng WK, Shen S, et al. Scalable ionic gelation synthesis of chitosan nanoparticles for drug delivery in static mixers. Carbohydr Polym 2013;94:940–945.
[38] Ji J, Hao S, Wu D, et al. Preparation, characterization and *in vitro* release of chitosan nanoparticles loaded with gentamicin and salicylic acid. Carbohydr Polym 2011;85:803–808.
[39] Liu C, Desai KGH, Chen X. Preparation and characterization of nanoparticles containing trypsin based on hydrophobically modified chitosan. J Agric Food Chem 2005;53:1728–1733.
[40] Wei Y, Gao Y, Xie Q. Isolation of chlorogenic acid from *Flaveria bidentis* (L.) Kuntze by CCC and synthesis of chlorogenic acid-intercalated layered double hydroxide. Chromatographia 2011;73:97–102.
[41] Alishahi A, Mirvaghefi A, Tehrani MR, et al. Shelf life and delivery enhancement of vitamin C using chitosan nanoparticles. Food Chem 2011;126:935–940.
[42] Derakhshandeh K, Fathi S. Role of chitosan nanoparticles in the oral absorption of Gemcitabine. Int J Pharm 2012;437:172–177.
[43] Amorim CM, Couto AG, Netz DJA, et al. Antioxidant idebenone-loaded nanoparticles based on chitosan and N-carboxymethylchitosan. Nanomed Nanotechnol Biol Med 2010;6:745–752.
[44] Ajun W, Yan S, Li G, et al. Preparation of aspirin and probucol in combination loaded chitosan nanoparticles and *in vitro* release study. Carbohydr Polym 2009;75:566–574.
[45] Zhou SB, Deng XM, Li XH. Investigation on novel core-coated microspears protein delivery systems. J Control Release 2001;75:27–36.
[46] Hu B, Pan C, Sun Y, et al. Optimisation of fabrication parameters to produce chitosan-tripoyphosphate nanoparticles for delivery of tea catechins. J Agric Food Chem 2008;56:7451–7458.